

Development of Micellar Novel Drug Carrier Utilizing Temperature-Sensitive Block Copolymers Containing Cyclodextrin Moieties

Firdaus Yhaya,^{†,‡} Johnny Lim,[†] Yoseop Kim,^{†,§} Mingtao Liang,[†] Andrew M. Gregory,[†] and Martina H. Stenzel^{*,†}

[†]Centre for Advanced Macromolecular Design (CAMD), School of Chemical Engineering, University of New South Wales, Sydney, NSW 2052, Australia

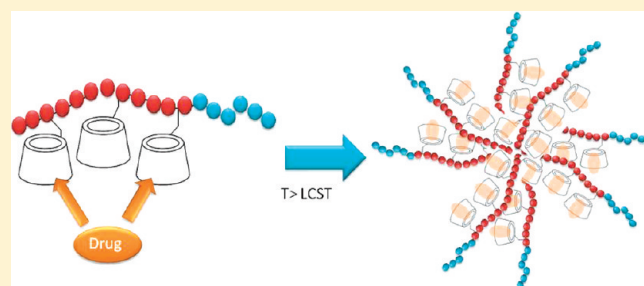
[‡]School of Industrial Technology, University Sains Malaysia, 11800 Minden, Penang, Malaysia

[§]Cancer Research Laboratories, Department of Surgery, St. George Hospital, University of New South Wales, Sydney, NSW 2217, Australia

S Supporting Information

ABSTRACT: A drug-delivery system for albendazole (ABZ) based on β -cyclodextrin has been synthesized. Well-defined statistical copolymers, composed of *N*-isopropylacrylamide (NIPAAm) and trimethylsilylpropargyl acrylate (TMSPA), have been prepared by reversible addition–fragmentation chain transfer (RAFT) polymerization. The reactivity ratios were determined to be $r_{\text{TMSPA}} = 1.12$ and $r_{\text{NIPAAm}} = 0.49$, in the absence of RAFT agent, and $r_{\text{TMSPA}} = 1.35$ and $r_{\text{NIPAAm}} = 0.35$, in the presence of RAFT agent using the average of different techniques. Block copolymers were prepared using a POEGMEA₄₀ macro-RAFT agent chain extended with NIPAAm and TMSPA in various feed ratios. After deprotection, the polymers were reacted with 6I-azido-6I-deoxy- β -cyclodextrin via Huisgen azide–alkyne 1,3-

dipolar cycloaddition, resulting in thermo-responsive block copolymers with pendant β -cyclodextrin groups, which were then acetylated to modify the polarity and inclusion-complex formation of β -cyclodextrin with the drug albendazole (ABZ). Only block copolymers with small amounts of cyclodextrin were observed to have an LCST while the copolymers containing higher β -cyclodextrin fractions increased the LCST of PNIPAAm beyond measurable temperature ranges. Encapsulation of ABZ increased the LCST. The loading efficiency increased in the polymer β -cyclodextrin conjugate compared to native β -cyclodextrin with the highest loading observed in the block copolymer after all remaining cyclodextrin hydroxyl groups had been acetylated. While β -cyclodextrin is toxic, attachment of a polymer lowered the toxicity to nontoxic levels. The ABZ-loaded polymers were all observed to be highly toxic to OVCAR-3 ovarian cancer cell lines with the acetylated polymer showing the highest toxicity.



1. INTRODUCTION

Recently, albendazole [ABZ, methyl(5-propylthio-1*H*-benzimidazol-2-yl)carbamate, Figure 1] has been identified as a potential systemic anticancer agent besides its normal use as an anthelmintic drug against human and animal parasites.^{1–8} However, ABZ has low aqueous solubility, which limits its use for the treatment of cancer.

In order to enhance the aqueous solubility of ABZ and its bioavailability, several strategies have been proposed in the literature. Cyclodextrins can be used to help solubilize poorly water-soluble species by the formation of “inclusion complexes” or “host–guest complexes” (Figure 1).^{9,10} Among several types of cyclodextrins, used to form inclusion complexes with ABZ, 2-hydroxypropyl- β -cyclodextrin was found to be useful in terms of bioavailability and complexation potential.^{11,12} The solubilization of ABZ in cyclodextrin polymers has been found to enhance

antiproliferative activity compared to native cyclodextrins alone.⁷ Despite the increase in solubility, this technique still required huge amount of cyclodextrins and the inclusion complexes were too small in size for drug delivery systems.

Nanoparticles based on cyclodextrin are widely investigated in order to combine the features of solubility enhancer with the enhanced permeation–retention effect (EPR) of nanoparticles.^{13–17} The EPR of nanoparticles allows passive targeting of drugs via the preferred lodgment of nanoparticles in the tumor while the lymphatic system of the tumor is not capable of clearing the polymer therefore, the drug carrier remains trapped. However, many of these “cyclodextrin polymers” are undefined since they

Received: June 20, 2011

Revised: September 12, 2011

Published: October 05, 2011

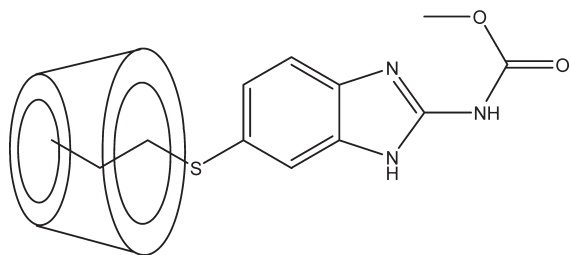


Figure 1. Inclusion complex of ABZ in cyclodextrin. The aliphatic part of ABZ was suggested to be responsible for the formation of the inclusion complex.¹⁰

were made by polycondensation of the native cyclodextrins leading to branching and often insoluble networks.¹⁸

Well-defined polymers with pendant cyclodextrin groups are rarely discussed in the literature, compared to the branched “cyclodextrin polymers”.¹⁸ The synthesis of cyclodextrin polymers using cyclodextrin monomers was first reported by Furue and co-workers in 1975.¹⁹ Although most of the polymers produced were homopolymers,¹⁸ in some cases copolymerizations were examined.^{18,20–25} Alternatively, postfunctionalization of a reactive linear polymer with monofunctional cyclodextrin was investigated.¹⁸ Seo et al.²⁶ were among the first to use the two-step polymer analogous reaction. An efficient route to polymers with pendant cyclodextrin has been developed by Ritter and co-workers using efficient Cu(I) catalyzed alkyne azide Huisgen cycloaddition (click reaction). Despite all the recent advancements in this area, the polymers were typically prepared via free radical polymerization and more complex architectures such as block copolymers are noticeably absent.

RAFT polymerization allows the precise control over the macromolecular architecture with structures such as block copolymers and other complex and elaborate architectures easily accessible through facile reactions.^{27–30} The effortless design of amphiphilic block copolymers via RAFT opens the door to new self-assembled structures including micelles, which are attractive nanomaterials for drug delivery.^{31–33} Poly(ethylene glycol) (PEG) is the polymer of choice to create the corona of the micelle to enhance circulation time of the drug carrier, although there are some indications that PEG might interact with proteins.³⁴ The design of the core of the micelle is inspired by the work of Ritter and co-workers who showed that the LCST of NIPAAm can be influenced by having cyclodextrin as a polymer building block. The changes in the LCST behavior is intrinsically linked to the type of guest.^{24,35} Upon loading of ABZ into β -cyclodextrin and heating of the block copolymer above the LCST of the block copolymer, micelles are expected to form.

EXPERIMENTAL SECTION

Materials. The synthesis of RAFT agent, 3-(benzylsulfanylthiocarbonylsulfanyl)propionic acid (3-BSPA), is described elsewhere.^{36,37} 3-Mercaptopropionic acid, carbon disulfide, benzyl bromide, *N*-isopropylacrylamide (NIPAAm), propargyl alcohol, acryloyl chloride, oligo(ethylene glycol) methyl ether acrylate (OEGMEA) of $M_n \sim 480$ g mol⁻¹, chlorotrimethylsilane (CTMS), silver chloride, anhydrous magnesium sulfate, 1,8-diazabicyclo[5.4.0]undec-7-ene (DBU), *p*-toluenesulfonyl chloride (PTSC), sodium azide, tetrabutylammonium fluoride (TBAF), silica gel, sodium azide, ascorbic acid, albendazole, acetic anhydride, pyridine, 4-dimethylaminopyridine (DMAP) were purchased from Sigma-Aldrich and used as received. 2,2'-azobis(isobutyronitrile)

(AIBN) was purified by recrystallization twice in methanol. Triethylamine was dried using molecular sieves overnight prior to use and β -cyclodextrin was recrystallized from water. Only copper sulfate was purchased from BDH. All solvents used were of analytical grade, except acetone and ethanol. Distilled water from Ultrapure was used throughout this work. All chemicals were used as received unless stated otherwise.

Synthesis and Methods. *Synthesis of Trimethylsilylpropargyl Acrylate (TMSPA).* The synthesis of TMSPA was carried out in a two-stage process. Propargyl acrylate (2-propynyl propenoate)³⁸ was synthesized first and later reacted with chlorotrimethylsilane to obtain TMSPA.³⁹ Initially, acryloyl chloride (8.42 mL, 1.03×10^{-1} mol) was added dropwise to a stirred solution of propargyl alcohol (5 mL, 8.60×10^{-2} mol) and triethylamine (14.4 mL, 1.03×10^{-1} mol) in dichloromethane (400 mL) at 0 °C. The clear solution turned yellow. The reaction mixture was allowed to reach room temperature where the color darkened. The mixture was stirred overnight and then quenched with saturated sodium hydrogen carbonate solution. The organic layer was extracted with 10% hydrochloric acid (3 \times 30 mL), saturated sodium hydrogen carbonate solution (1 \times 30 mL), and water (1 \times 30 mL), dried over magnesium sulfate, filtered through neutral alumina, concentrated *in vacuo* to obtain green/yellow propargyl acrylate (87% yield). In the second stage, silver chloride (1.56 g, 1.06×10^{-2} mol) was suspended in 154 mL of dry dichloromethane. Propargyl acrylate (12.4 mL, 1.12×10^{-1} mol) and DBU (21.4 mL, 1.43×10^{-2} mol) were added to this suspension. A dark red color was observed. The reaction mixture was then heated to 40 °C and chlorotrimethylsilane (21.2 mL, 1.59×10^{-1} mol) was added dropwise and stirring continued for the next 24 h. The dark solution obtained was diluted with *n*-hexane (400 mL) and the organic phase was washed successively with saturated aqueous sodium hydrogen carbonate, hydrochloric acid (1%) and water, dried over magnesium sulfate, filtered, and concentrated *in vacuo*. The crude product obtained was purified by column chromatography eluting with a 25:1 mixture of *n*-hexane and diethyl ether to obtain colorless trimethylsilylpropargyl acrylate liquid (36.7% yield). $R_f = 0.71$.

Synthesis of the PNIPAAm and PTMSPA Homopolymers. NIPAAm was recrystallized from *n*-hexane and 2,2'-azobis(isobutyronitrile) (AIBN) was recrystallized twice from methanol. NIPAAm (3.39 g, 3.00×10^{-2} mol) was mixed with RAFT agent (3-BSPA) (32.6 mg, 1.20×10^{-4} mol) inside a Schlenk tube. A stock solution of 1.20×10^{-5} mol L⁻¹ of AIBN with *N,N*-dimethylacetamide (DMAc) was prepared and 10 mL of this solution was added to the Schlenk tube. The tube was sealed and degassed using five freeze–pump–thaw cycle. The polymerization mixture was immersed in an oil bath at 60 °C for different time intervals. The polymers were analyzed using NMR and SEC analyses to determine monomer conversion and molecular weight, respectively. For the synthesis of PTMSPA homopolymer, TMSPA (5.46 g, 3.00×10^{-2} mol) of was used, but other parameters and conditions were similar as of synthesis of PNIPAAm homopolymer.

*Synthesis of P(NIPAAm-*s*-TMSPA) Statistical Copolymers.* Statistical copolymers P(NIPAAm-*s*-TMSPA) were prepared similar to the procedures above by varying the feed ratios between NIPAAm and TMSPA monomers. The molar ratios were [NIPAAm]:[TMSPA] = 80:20, [NIPAAm]:[TMSPA] = 90:10, and [NIPAAm]:[TMSPA] = 95:5. The total monomer concentration for each copolymer system was kept at 3 mol L⁻¹. For the synthesis of the copolymer with the feed ratio of [NIPAAm]:[TMSPA] = 80:20, NIPAAm (2.71 g, 2.40×10^{-2} mol), TMSPA (1.09 g, 6.00×10^{-3} mol), 3-BSPA RAFT agent (32.0 mg, 1.20×10^{-4} mol), and AIBN (1.97 mg, 1.20×10^{-5} mol) were added to 10 mL of DMAc. After the monomer conversion and molecular weight had been determined, the polymer were purified by dialysis using tubular membranes with a molecular weight cutoff (MWCO) of 3 500 Da for 2 days in ethanol to remove TMSPA and 2 days in water to remove NIPAAm. The copolymers were then freeze-dried.

Synthesis of POEGMEA macro-RAFT Agent. In a 100 mL round-bottomed flask, OEGMEA (3.46 g, 7.20×10^{-3} mol) was polymerized in toluene (2.4 mL) at 60 °C in the presence of the RAFT agent 3-BSPA (32.6 mg, 1.20×10^{-4} mol) and AIBN (1.97 mg, 1.20×10^{-5} mol). The molar ratio used was [OEGMEA]:[RAFT agent 3-BSPA]:[AIBN] = 60:1:0.1. The solution was purged with nitrogen for 45 min and the polymerization was carried out for 3 h to obtain 44% conversion by NMR. The POEGMEA macro-RAFT agent was purified by dialysis against methanol to obtain a yellow viscous liquid.

Theoretical number-average molecular weight calculated using conversion $M_{n(\text{theo})} = 19\,200 \text{ g mol}^{-1}$. Size exclusion chromatography (SEC) determined number-average molecular weight $M_{n(\text{SEC})} = 20\,600 \text{ g mol}^{-1}$, PDI: 1.23 (polystyrene standards).

Synthesis of POEGMEA-*b*-P(NIPAAM-*s*-TMSPA) Block Copolymer. The chain extension was carried out according to the method described for P(NIPAAM-*s*-TMSPA) by replacing 3-BSPA with POEGMEA macro-RAFT agent. The molar ratios [NIPAAM]:[TMSPA] = 80:20, [NIPAAM]:[TMSPA] = 90:10, and [NIPAAM]:[TMSPA] = 95:5 were employed. For ratio of [NIPAAM]:[TMSPA] = 80:20, NIPAAM (2.71 g, 2.40×10^{-3} mol), TMSPA (1.09 g, 6.00×10^{-3} mol), POEGMEA macro-RAFT agent (2.30 g, 1.20×10^{-4} mol), and AIBN (1.97 mg, 1.20×10^{-5} mol) were added to 10 mL of DMAc. The samples were then treated as described above. The block copolymers were purified by dialysis in ethanol and then water followed by freeze-drying.

Deprotection of Copolymers. The cleavage of the trimethylsilyl protecting group was carried out according to the method by Ladmiral et al.⁴⁰ with modifications to the amount of acetic acid and TBAF used and the time taken to complete the reaction. The trimethylsilyl protected polymer (150 mg) and acetic acid (2.0 equiv mol/mol with respect to the alkyne–trimethylsilyl groups) were dissolved in THF (10 mL). Nitrogen was purged through the solution (ca. 20 min) and then cooled to 0 °C. A 1 M solution of tetrabutylammonium fluoride (TBAF·3H₂O) in THF (2.0 equiv mol/mol with respect to the alkyne–trimethylsilyl groups) was added slowly via syringe (ca. 2–3 min). The resulting turbid mixture was stirred at this temperature for 30 min and then warmed to ambient temperature. The deprotection was complete after 48 h, and the reaction solution was passed through a short silica pad in order to remove excess TBAF and the pad was subsequently washed with additional THF. The resulting solution was then concentrated under reduced pressure, diluted in chloroform, and the polymer was precipitated in petroleum ether 40–60 °C before centrifugation. The copolymer was dissolved in DMAc and dialyzed in dialysis tube 3500 MWCO for 4 days against water, followed by freeze-drying.

Synthesis of 6I-Azido-6I-deoxy- β -cyclodextrin. β -Cyclodextrin was monotosylated before azidification to obtain 6I-azido-6I-deoxy- β -cyclodextrin (β -CD azide).⁴¹ Recrystallized β -cyclodextrin (63.3 g, 5.00×10^{-2} mol) was suspended in 500 mL water and stirred. A 5.65 g sample of NaOH was dissolved in 20 mL of water and added dropwise into the β -cyclodextrin solution. Meanwhile, *p*-toluenesulphonyl chloride (PTSC) (9.50 g, 6.00×10^{-2} mol) was dissolved in 30 mL of acetonitrile, and later also added dropwise into the β -cyclodextrin solution. A white precipitate was observed immediately. The reaction was run overnight and the white solid was filtered and dried in the vacuum oven at 30 °C overnight. A yield of 4.43 g of mono-6-*p*-toluenesulfonyl- β -cyclodextrin was obtained. For the azide formation, dried mono-6-*p*-toluenesulfonyl- β -cyclodextrin (4.21 g, 3.26×10^{-3} mol) was reacted with 5 equiv of sodium azide in 20 mL of anhydrous DMF at 80 °C overnight. The solution was precipitated in acetone and dried under vacuum at 30 °C to obtain 6I-azido-6I-deoxy- β -cyclodextrin (β -cyclodextrin azide). ¹H NMR (DMSO-*d*₆): δ 6.0–5.90 (14H, OH-2, OH-3), 4.97 (d, 1H, H₁), 4.95–4.88 (m, 6H, H_{1II-VI}), 4.67–4.53 (m, 6H, OH-6), 3.90–3.60 (m, 28H, H₃, H₅, H₆), 3.5–3.35 (m, 14H, H₄, H₂).

Huisgen Azide–Alkyne 1,3-Dipolar Cycloaddition Model Reaction between β -Cyclodextrin Azide and Propargyl Alcohol. In order to

study the feasibility of the reaction of β -cyclodextrin azide onto the copolymer, a model reaction was carried out. Propargyl alcohol was reacted with β -cyclodextrin azide in DMF. 1.00×10^{-3} mol (5.61 g) of propargyl alcohol and 1.00×10^{-3} mol (1.16 g) of β -cyclodextrin azide were dissolved together in 10 mL of DMF. The reaction flask was sealed with a rubber septum and the solution was stirred under a nitrogen atmosphere for 24 h at 100 °C. The product was collected after precipitating the solution into 100 mL of acetone followed by filtration. The liquid phase was dialyzed for 4 days in water and freeze-dried. The dried product was analyzed by ¹H NMR in DMSO-*d*₆.

Huisgen Azide–Alkyne 1,3-Dipolar Cycloaddition Reaction between β -Cyclodextrin Azide and Polymer. For the reaction of β -cyclodextrin azide with various copolymers, two systems were tested: the traditional Huisgen azide–alkyne 1,3-dipolar cycloaddition without catalyst and the Cu(I) catalyzed approach (*click chemistry*), which was carried out according to the method described by Munteanu et al.⁴² The nickel system employed similar conditions as the model reaction.

¹H NMR (DMSO-*d*₆): δ 5.73 (OH-3, OH-4), 4.84 (H₁), 4.5 (OH-6), 4.1 (CH₂-N, CO-O-CH₂), 3.8 (CH(CH₃)₂, H₅, H₆), 3.5 (-O-CH₂-CH₂-O, H₄, H₂), 1.5–2.3 (CH backbone), 1.0 (CH(CH₃)₂).

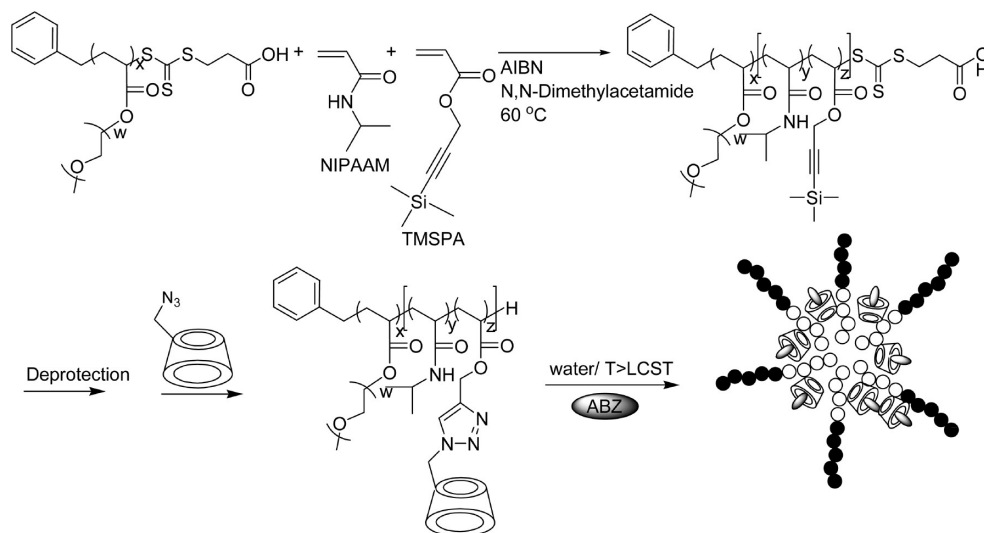
Acetylation of Copolymer. 20 mg of copolymer was mixed together with 1 mL of acetic anhydride, 2 mL of pyridine in a round-bottomed flask and 1 mg of DMAP was added as catalyst. The solution was stirred at 50 °C for 24 h and dialyzed in dialysis tube 6000–8000 MWCO for 4 days with frequent water changes, followed by freeze-drying for 48 h. ¹H NMR (DMSO-*d*₆): δ 4.8 (H₁), 4.1 (CH₂-N, CO-O-CH₂), 3.8 (CH(CH₃)₂, H₅, H₆), 3.5 (-O-CH₂-CH₂-O, H₄, H₂), 2.1 (CH₃-C=O), 1.5–2.3 (CH backbone), 1.0 (CH(CH₃)₂).

Measurement of Drug Loading Efficiency on Polymeric Micelles. Initially, 20 mg of the β -cyclodextrin/copolymer and ABZ (mole ratio of β -cyclodextrin moieties:ABZ = 1:1) were dissolved in 4 mL of water and 4 mL of THF (or acetone) separately. Both solutions were then mixed. Water was added slowly and stopped as soon as precipitate started forming. The water addition step is crucial in creating an aqueous environment for ABZ, by doing so the ABZ is pushed into the β -cyclodextrin cavities, forming the inclusion complexes. Omitting this step would result in zero loading, as proven by ¹H NMR (result not shown). After 24 h of stirring at room temperature, THF was slowly removed by vacuum. The unloaded drug was removed by means of passing the solution through 0.45 μ m filter and subsequently the sample was freeze-dried for 48 h. For loading analysis via ¹H NMR, equimolar ratio of adamantane methanol to β -cyclodextrin moieties was added, and whole system was dissolved in deuterated DMSO (DMSO-*d*) with 0.5 μ L of styrene added as an internal standard. Styrene of known concentrations was used to determine the concentration of ABZ by comparing the integrals of styrene with the ABZ integrals. The loading was determined from the vinylic peak of styrene (-C=CH₂, δ = 5.7–6.0) and the ABZ -CH₂-CH₂ peak (δ = 2.8–3.2). The drug loading efficiency (DLE) was calculated according to

$$\text{DLE (\%)} = \frac{\text{amount of ABZ in micelle}}{\text{amount of ABZ added initially}} \times 100$$

Other internal standards can be applied as long as they do not overlap with existing signals. Addition of adamantane methanol is recommended to compete with ABZ for the cavity. The released ABZ was found to have clearer and more intensive ¹H NMR signals.

In Vitro Cytotoxicity Tests. Human ovarian cancer OVCAR-3 cells were seeded in 96-well plates (3 000 cells per well) with culture medium 10% RPMI-1640 [2×10^{-3} M L-glutamine, 1.5 g L⁻¹ sodium bicarbonate, 0.010 M of 2-hydroxyethylpiperazinesulfonic acid (HEPES), 4.5 g L⁻¹ glucose, 1.00×10^{-3} M sodium pyruvate at 37 °C in 5% CO₂ environment for 24 h. The medium was refreshed with 0.2 mL of a solution consisting of 0.1 mL medium and 0.1 mL of micelle solution of

Scheme 1. Schematic Approach to Thermo-Responsive Micelles Based on Block Copolymers with Pendant β -Cyclodextrin

P(NIPAAm₁₁₆-*b*-PA- β -cyclodextrin₄₃), POEGMEA₄₀-*b*-P(NIPAAm₁₅₀-*b*-PA- β -cyclodextrin₁₁) and acetylated POEGMEA₄₀-*b*-P(NIPAAm₁₅₀-*b*-PA- β -cyclodextrin₁₁) micelles with and without ABZ loading to reach a final micelle concentration of 62.5, 125, 250, and 500 $\mu\text{g mL}^{-1}$, respectively, followed by incubation at 37 °C in the incubator for 72 h. Subsequently, the medium was removed and washed 5 times with tap water and 5 times with 1% acetic acid. After drying overnight, 100 μg of 0.010 M Tris (pH = 10.5) was added to solubilize the dye. Absorbance was measured at 570 nm using Σ 960 platereader (Metertech, Taiwan). Nontreated cells were used as controls. The absorbance was measured at 570 nm and the optical density (OD) was used to calculate cell viability [cell viability (%) = (test – blank)/(control – blank) x 100]:

$$\text{cell viability (\%)} = \frac{[(\text{OD}_{570, \text{sample}} - \text{OD}_{570, \text{blank}}) / \text{OD}_{570, \text{control}} - \text{OD}_{570, \text{blank}}]}{1} \times 100$$

Self-Assembly and Thermal Properties of Micelles. Solutions of both ABZ loaded and unloaded copolymers were prepared at a concentration of 1 mg mL⁻¹ in water. The solution was placed in a quartz cuvette after being passed through a 0.45 μm filter to remove the particle impurities. The cuvette was placed in a dynamic light scattering (DLS) particle size analyzer. The temperature was increased slowly from 20 to 80 °C, with a 5 min stabilization period before measurement at each temperature. The change of the average particles diameters or mean count rate vs temperature was then observed. The temperature where scattering intensity drastically increased (cloud point) was taken as the LCST of the copolymers being tested. Transmission electron microscopy (TEM) was also used to observe the formation of micelles.

Analysis. *NMR Spectroscopy.* NMR spectra were recorded using a Bruker 300 MHz spectrometer; samples were analyzed in CDCl₃ and DMSO-*d*₆ at 25 °C. For the determination of reactivity ratios, testing of solvent choice and optimization of the NMR experiment were vital preliminary experiments. The solvent DMSO-*d*₆ and an ¹H NMR relaxation time of 1 s were deemed suitable.

FT-IR Spectroscopy. The FT-IR spectra were recorded on a Perkin-Elmer FT-IR spectrometer. The scanning range was 400–4000 cm⁻¹ and the resolution was 1 cm⁻¹.

Electrospray Ionization Mass Spectrometry (ESI-MS). ESI-MS was used to confirm the existence of mono-6-*p*-toluenesulfonyl- β -cyclodextrin and 6I-azido-6I-deoxy- β -cyclodextrin. Each sample was freshly prepared before analysis by dissolving the product in a 1:1 solution of water:

methanol with concentration of 1 mg/mL and filtered with 0.45 μm filter. Mass spectrometry analyses were undertaken with a Thermo Finnigan LCQ Deca quadruple ion trap mass spectrometer (Thermo Finnigan, San Jose, CA), equipped with an atmospheric pressure ionization source operating in the nebulizer assisted electrospray mode and was used in positive ion mode. Mass calibration was performed using caffeine, MRFA and Ultramark 1621 (Aldrich) in the *m/z* range of 195–1822 Da. All spectra was acquired within the *m/z* range of 150–2000 Da, and typical instrumental parameters were a spray voltage of 4.5 kV, a capillary voltage of 44 V, a capillary temperature of 275 °C and flow rate of 5 $\mu\text{L}/\text{min}$. Nitrogen was used as sheath gas (flow: 50% maximum) and helium was used as auxiliary gas (flow: 5% maximum). 30 microscans, with maximum inject time of 10 ms per microscan, were performed. For each respective scan, approximately 35 scans were averaged to obtain the final spectrum. The solvent used was a 3:1 mixture of dichloromethane:methanol with sodium acetate concentration of 0.3 μM . Sodium acetate was added to the solvent prior to analyses to ensure ionization and to suppress potassium salt peaks. All theoretical molecular weights were calculated using the exact mass for the first peak in any given isotopic pattern. The molecular weights of the most abundant isotopes were calculated using the following values: C¹² = 12.000000; H¹ = 1.007825; O¹⁶ = 15.994915; Na²³ = 22.989768.

Size Exclusion Chromatography (SEC). Molecular weight distributions of the copolymer systems were determined by means of SEC using a Shimadzu modular system, comprising an autoinjector, a Polymer Laboratories (PL) 5.0 μm bead-size guard column (50 × 7.5 mm²), followed by three linear PL columns (10⁵, 10⁴, 10³) and a differential-refractive-index detector. The eluent was DMAc (0.05% w/v LiBr, 0.05% 2,6-dibutyl-4-methylphenol) at 50 °C with a flow rate of 1 mL min⁻¹. The system was calibrated using narrowly dispersed polystyrene standards ranging from 500 to 10⁶ g mol⁻¹. The polymer (5 mg) was dissolved in 2 mL DMAc, followed by filtration using a filter with a pore size of 0.45 μm .

Dynamic Light Scattering (DLS). Hydrodynamic diameters of copolymers in water were obtained using a Brookhaven Zetaplus particle size analyzer. Samples were filtered before analyzing and the temperature range used was from 20 to 80 °C.

Transmission Electron Microscopy (TEM). The TEM micrographs were obtained using a JEOL 1400 transmission electron microscope. The instrument operates at an accelerating voltage of 100 kV. Samples were negative stained with phosphotungstic acid (2 wt %). A Formvar-coated grid was coated by casting a polymer aqueous solution for 1 min. Excess solution was removed using filter paper. For staining, a drop of

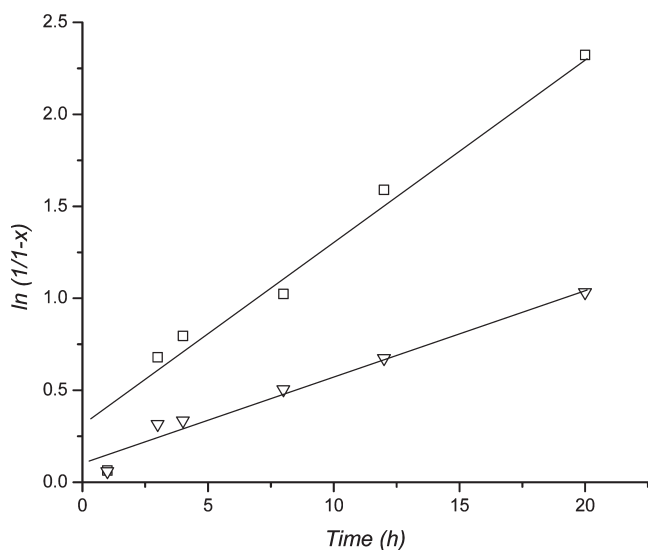
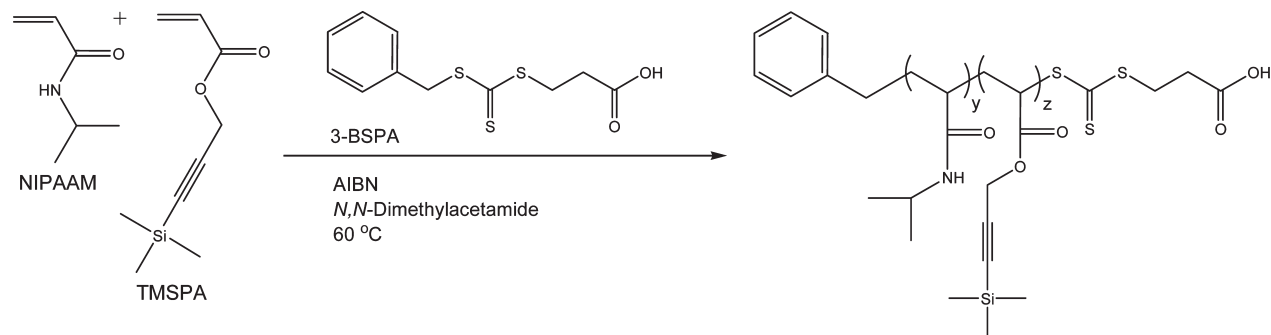
Scheme 2. Synthesis of P(NIPAAM-*s*-TMSPA) Statistical Copolymer

Figure 2. Pseudo first order kinetic plot showing the consumption of TMSPA (square) and NIPAAM (triangle) of the copolymerization of both monomers at 60 °C in DMAc in the presence of RAFT agent 3-BSPA ($[M] = 3 \text{ mol L}^{-1}$, $[AIBN] = 1.2 \times 10^{-3} \text{ mol L}^{-1}$, $[RAFT \text{ agent } 3\text{-BSPA}] = 1.2 \times 10^{-2} \text{ mol L}^{-1}$, $[TMSPA]:[NIPAAM] = 5:95$).

phosphotungstic acid was gently applied onto the surface of the grid for 30 s. The stained grid was dried in air.

RESULTS AND DISCUSSION

RAFT polymerization was chosen to construct the copolymers due to its simplicity and easy control of polymer architecture. Concerns about the toxicity of thiocarbonylthio RAFT end group should be dismissed as the deprotecting stage and dialysis remove this group irreversibly. Before any block copolymer synthesis as outlined in Scheme 1 was attempted, a detailed study on the RAFT polymerization for the homopolymerization of PNIPAAM and TMSPA and their respective copolymerization was carried out. *N,N*-Dimethylacetamide (DMAc) was chosen as the solvent for the polymerization. It was found that the DMAc dried in magnesium sulfate gave better reproducibility as compared to the DMAc dried in molecular sieves. The polymerization of NIPAAM using 3-BSPA was reported earlier.⁴⁵ The comonomer, TMSPA, was homopolymerized using the same RAFT agent resulting in polymers with reasonably low molecular weight distribution, although a hybrid behavior between RAFT and free

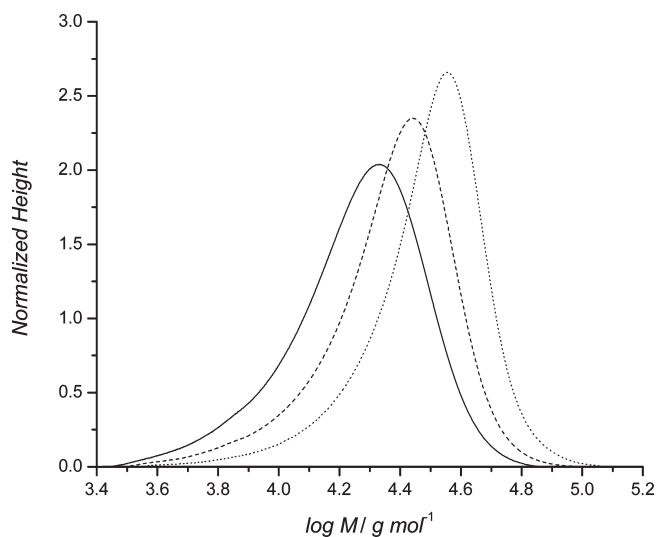


Figure 3. Molecular weight distribution obtained from SEC of the copolymerization of NIPAAM and TMSPA at 60 °C. ($[M] = 3 \text{ mol L}^{-1}$, $[RAFT \text{ groups}] = 1.20 \times 10^{-2} \text{ mol L}^{-1}$, $[AIBN] = 1.20 \times 10^{-3} \text{ mol L}^{-1}$ in *N,N*-dimethylacetamide). From left to right, the molar ratios between $[TMSPA]:[NIPAAM]$ were 20:80, 10:90, and 5:95.

radical polymerization is observed indicating a sluggish addition of the macroradical to the RAFT agent (Figure S1, Supporting Information). The copolymerization of NIPAAM and TMSPA was subsequently investigated in detail at various feed ratios ($f_{TMSPA} = 5, 10$ and 20%) to establish the distribution of both monomers along the polymer chain (Scheme 2). In general, the rate of polymerization declined with increasing amounts of TMSPA (Figures S2 and S3, Supporting Information). The consumption of both monomers was monitored independently via NMR showing a preference for TMSPA in all cases with a typical example displayed in Figure 2 (see as Table S1, Figures S2 and S3, Supporting Information, for details).

The polymers obtained as a result of the copolymerization were all observed to have PDIs of approximately 1.3. The difference between predicted and experimental molecular weights was very likely due to the SEC calibration using polystyrene standards (Figure 3, Table S1, Supporting Information). Figure 3 displays typical molecular weight distributions obtained from statistical polymers P(NIPAAM₁₁₆-*s*-TMSPA₄₃), P(NIPAAM₈₄-*s*-TMSPA₃₁), and P(NIPAAM₅₄-*s*-TMSPA₁₉), which were generated after a polymerization time of 20 h with molar feed ratios of

Table 1. Reactivity Ratios Obtained by Different Approaches

reactivity ratio	free radical polymerization		RAFT polymerization	
	r_1	r_2	r_1	r_2
Fineman Ross	1.22	0.56	1.48	0.41
Kelen Tüdös	0.95	0.45	1.22	0.31
Mayo Lewis	1.19	0.51	1.30	0.31
CONTOUR	1.12	0.46	1.40	0.36
average	1.12	0.47	1.35	0.35

$f_{\text{TMSPA}} = 0.05, 0.1$ and 0.2 , respectively (Table S1, Supporting Information).

According to these initial results, the copolymer should have a gradient structure with the enrichment of TMSPA in the beginning of the polymerization. To quantify this observation, the reactivity ratios of this copolymerization in the presence and absence of the RAFT agent were determined. The monomer feed ratios were varied from $f_{\text{NIPAAM}} = 0.1$ to $f_{\text{NIPAAM}} = 0.9$ in 0.1 increments, hence, resulting in a set of nine samples. To achieve a monomer conversion below 5%, imperative for a reactivity ratio study, the free radical polymerization was stopped at 1 h or less while the presence of the RAFT agent required a reaction time of 3 h due to an inhibition period (Figures S2 and S3, Supporting Information). The composition of the polymers after purification was determined using ^1H NMR spectrum as outlined in Figure S4, Supporting Information. Detailed calculations to determine F_{NIPAAM} , the composition of the polymer, can be found in the Supporting Information.

The mole fractions gathered from the NMR spectrum was used to calculate reactivity ratios. Of the four salient methods, Fineman Ross, Kelen Tüdös, Mayo Lewis, and the program CONTOUR,^{44,45} the latter three methods yielded harmonious results, despite having incomparable calculation approaches (Table 1). The program CONTOUR, implemented by van Herk, is generally recommended by IUPAC.⁴⁶

The reactivity ratios suggest that in both polymerization systems, free radical and RAFT, TMSPA (r_1) chain ends have a slight tendency to homopropagation ($r_1 \geq 1$). NIPAAM (r_2) is slightly inclined to cross propagate in RAFT, thus, the slight gradient structure of the polymer. The differences between free radical polymerization and RAFT polymerization are not significant, but visible. Similar to the finding by Barner-Kowollik and co-workers, the polymer mole fraction of the monomer with the larger reactivity ratio is increased in RAFT polymerization compared to the conventional copolymerization.⁴⁶ In summary, as observed by the consumption of the individual monomers, the initial stages of the polymerization consume more TMSPA, therefore an enrichment of TMSPA can be found at the α -terminal of the polymer chain, where the R-group is positioned. The composition drift can be visualized by calculating cumulative F using the measured reactivity ratios (Figure S6, Supporting Information).

Subsequently, block copolymers were prepared using OEGMA as the building block due to the biocompatible properties of the resulting polymer (Scheme 3). Before chain extension of P(OEGMEA) macro-RAFT agent with NIPAAM and TMSPA, POEGMEA homopolymer synthesis was achieved using 3-BSPA at 60 °C in DMAc as a solvent. After 3 h of reaction time, P(OEGMEA)₄₀ homopolymer with a theoretical molecular weight of 19 200 g mol⁻¹ and a narrow molecular weight distribution

with polydispersity index (PDI) of 1.23 was achieved, again suggesting a controlled living system. Purification was carried out via dialysis against methanol as the trial precipitation with *n*-hexane failed.

As outlined in Scheme 3, POEGMEA₄₀ macro-RAFT was utilized in a mixture with NIPAAM and TMSPA, using similar reaction conditions as employed in the copolymerization, to generate block copolymers. From the SEC curves in Figure 4, the absence of byproduct and narrow PDI between 1.16 and 1.36 suggested the polymerization proceeded in a living manner. The purification processes used for these block copolymers were similar to the statistical copolymers. Akin to the copolymerizations, the three mol ratios of $f_{\text{NIPAAM}} = 95, 90$ and 80% were employed leading after a reaction time of 20 h to the block copolymers POEGMEA₄₀-*b*-P(NIPAAM₁₅₀-*s*-TMSPA₁₁), POEGMEA₄₀-*b*-(NIPAAM₁₃₇-*s*-TMSPA₁₈), and POEGMEA₄₀-*b*-(NIPAAM₁₁₅-*s*-TMSPA₂₄), respectively. The molecular weights were in good agreement with the theoretical value while the SEC curves showed monomodal distributions. In contrast to the copolymerization using a low molecular weight RAFT agent, the rate of polymerization of TMSPA and NIPAAM in the presence of the macro-RAFT agent was less affected by the monomer composition (Table 2). With increasing amount of TMSPA only a slight drop in the rate of polymerization has been observed. The reason is the lowered consumption of TMSPA, compared to the copolymerization. The influence of the macro-RAFT agent on the reactivity ratio of the subsequent copolymerization has been described earlier as “bootstrap” effect.⁴⁷ The hydrophilic macro-RAFT agent has a preferred accumulation of hydrophilic NIPAAM around the active RAFT end-group leading to the increased consumption of the faster propagating NIPAAM. Comparison of actual compositions of the polymer with the calculated composition using the reactivity ratios in Table 1 (Figure S5, Supporting Information) show the incorporation of TMSPA has been delayed in the block copolymerization.

Huisgen Azide–Alkyne 1,3-Dipolar Cycloaddition with 6I-Azido-6I-deoxy- β -cyclodextrin. Prior to reaction of 6I-azido-6I-deoxy- β -cyclodextrin, the polymers were deprotected using tetrabutylammonium fluoride. The polymer lost its color due to the cleavage of the RAFT group during the procedure, probably replaced by a hydrogen as earlier mass spectroscopy analysis indicated.⁴⁸ NMR analysis confirmed the efficient removal of the protective group and the loss of the RAFT end group yielding POEGMEA-*b*-P(NIPAAM-*s*-PA) (Figure 5). A procedure from the literature has been adopted for the Huisgen azide–alkyne 1,3-dipolar cycloaddition (Scheme 4) using a copper-catalyzed *click* system using copper(II) sulfate pentahydrate/ascorbic acid at 140 °C.⁴² However, full copper removal was deemed impossible. Several procedures were attempted from removal via silica gel, extensive dialysis, to using a thiol complex and to washing with EDTA. After significant product loss, the seemingly colorless product was found to have still traces of Cu(I) ions, which were observed to be cytotoxic. Therefore, the traditional Huisgen azide–alkyne 1,3-dipolar cycloaddition in the absence of any catalyst was employed. A model reaction between 6I-azido-6I-deoxy- β -cyclodextrin and propargyl alcohol at 100 °C resulted in complete reaction after 24 h with, as expected, the formation of two stereoisomers as evidenced via NMR (Figure S7).

After the successful model reaction, four polymers—one statistical polymer, P(NIPAAM₁₁₆-*s*-PA₄₃) and the three block copolymers listed in Table 2—were reacted with 6I-azido-6I-deoxy- β -cyclodextrin. The modification process was confirmed

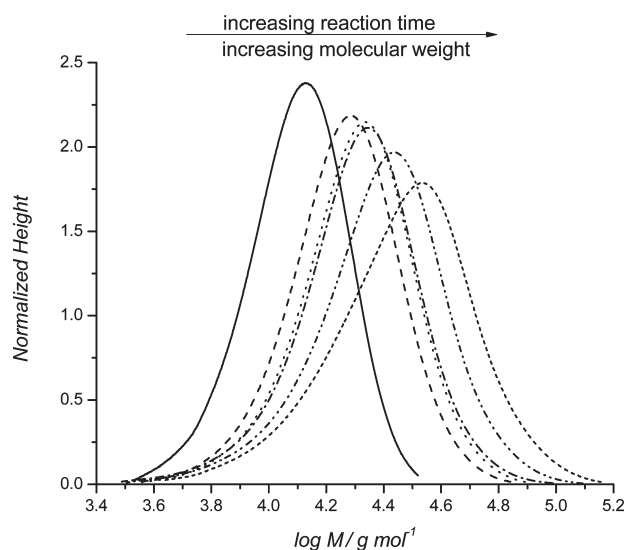
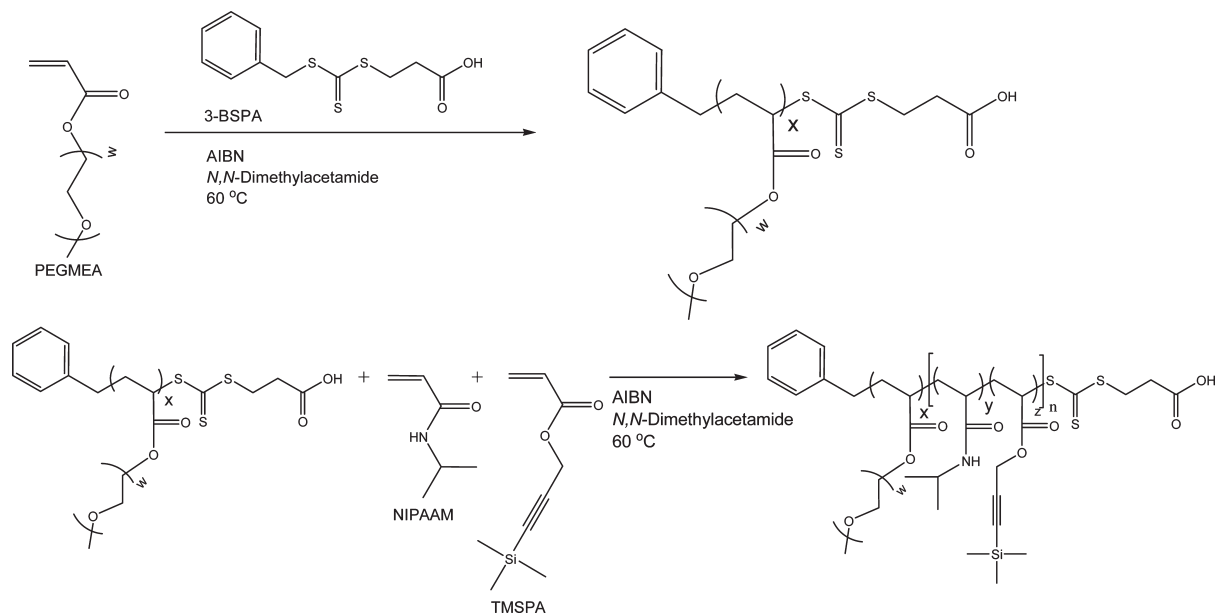
Scheme 3. Synthesis of POEGMEA-*b*-P(NIPAAM-*s*-TMSPA) Block Copolymer

Figure 4. Molecular weight distribution obtained from SEC of the block copolymerization of NIPAAM and TMSPA ($f_{\text{NIPAAM}} = 95\%$) at 60 °C with the presence of POEGMEA macro-RAFT agent. ($[M] = 3 \text{ mol L}^{-1}$, $[\text{RAFT groups}] = 1.20 \times 10^{-2} \text{ mol L}^{-1}$, $[\text{AIBN}] = 1.20 \times 10^{-3} \text{ mol L}^{-1}$ in *N,N*-dimethylacetamide. The polymerization times of the curves shown are 0, 4, 8, 12, 24, and 48 h.

by ^1H NMR (Figure 5), FT-IR (Figure S8, Supporting Information), and SEC (Figure 6). SEC traces from Figure 6 shows that the SEC curves are monomodal and high molecular weight shoulders are absent suggesting that no linkages formed between polymer chains. This reinforces the purity of 6I-azido-6I-deoxy- β -cyclodextrin and the presence of bifunctional cyclodextrin can be assumed absent. It should be noted here that the results for both block copolymers and statistical polymers are similar, unless stated otherwise. From ^1H NMR analysis, the modification process with 6I-azido-6I-deoxy- β -cyclodextrin was observed to be complete. The $-\text{CH}_2-$ signal of the propargyl ester before

modification (4.7 ppm) shifted to 4.2 ppm after reaction (Figure 5). Even though the peaks assigned to the proton in the triazole ring (7.9–8.4 ppm) appeared in the spectrum of model reaction, these peaks were not detected in the polymer peaks, possibly due to increased relaxation times. In order to confirm that the cyclodextrin peaks were not from free (unreacted) β -cyclodextrin azide, the polymer was dialyzed for 7 days in water using a tubular dialysis membrane with a molecular weight cutoff of 6000–8000 Da. FT-IR analysis of 6I-azido-6I-deoxy- β -cyclodextrin exhibited a sharp peak at 2000 cm^{-1} assigned to the azide functional group, which disappeared after reaction. The broad peak at $3000\text{--}3500 \text{ cm}^{-1}$ is indicative for the hydroxyl groups of cyclodextrin, which were absent before reaction (Figure S8, Supporting Information). The SEC confirmed the increase of the molecular weight of monomodal peak of POEGMEA-*b*-(NIPAAM-*s*-PA) to the higher molecular weight of POEGMEA-*b*-P(NIPAAM-*s*-PA- β -cyclodextrin) (Figure 6). Interestingly, there are no significant weight differences between the product obtained via Huisgen azide–alkyne 1,3-dipolar cycloaddition with and without Cu(I) catalyst.

The statistical polymers prior to β -cyclodextrin modification are insoluble in water while the block copolymers have clearly amphiphilic properties. The presence of TMSPA or, after deprotection, propargyl acrylate clearly lowers the water solubility of PNIPAAM. With conjugation of the hydrophilic β -cyclodextrin, the polymers become fully water-soluble. The presence of a comonomer will ultimately affect the lower critical solution temperature (LCST) of PNIPAAM.⁴⁹ The LCST of all polymers was determined via dynamic light scattering (DLS) using the scattering intensity as a means of determining the temperature. The onset of the increase coincides with the formation of more and bigger particles due to precipitation or micelle formation (Figure 7). The hydrophobic comonomer TMSPA lowered the LCST in all cases to such an extent that these polymers are insoluble in water at room temperature. In contrast, after reaction with 6I-azido-6I-deoxy- β -cyclodextrin, the LCST increased to

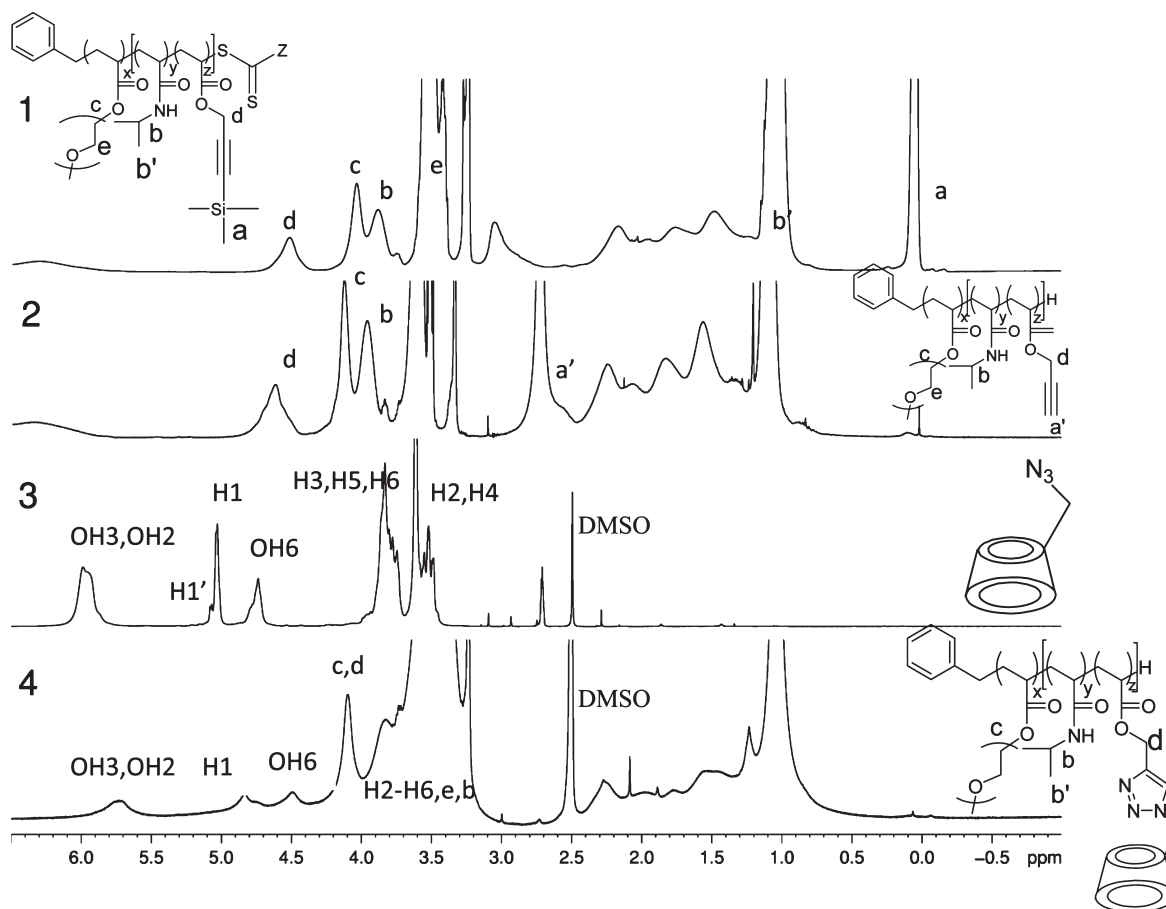
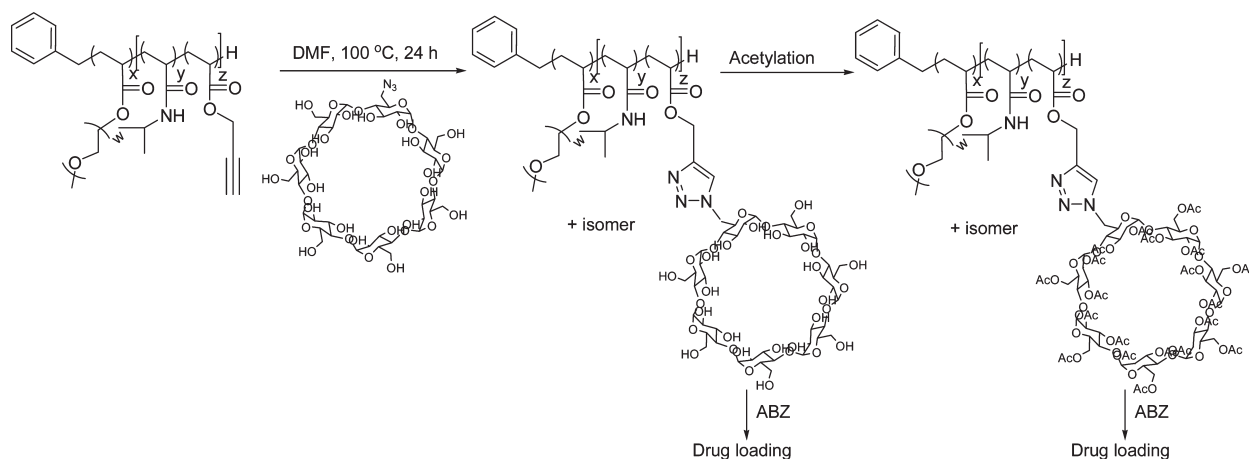


Figure 5. ^1H NMR analysis of POEGMEA₄₀-*b*-P(NIPAAm₁₁₅-*s*-TMSPA₂₄) before deprotection (A) and after deprotection (B), 6I-azido-6I-deoxy- β -cyclodextrin (C), and POEGMEA₄₀-*b*-P(NIPAAm₁₁₅-*s*-PA- β -cyclodextrin₂₄) (D). ^1H NMR spectra for 1 and 2 were obtained in CDCl₃, while spectra for 3 and 4 were obtained in deuterated DMSO.

Scheme 4. Huisgen Azide–Alkyne 1,3-Dipolar Cycloaddition with 6I-Azido-6I-deoxy- β -cyclodextrin and Subsequent Acetylation



temperatures of well above the LCST of PNIPAAm. The LCST of the statistical copolymer increases with increasing fraction of β -cyclodextrin in agreement with earlier studies.^{24,25,50} Interesting is the behavior of the prepared block copolymers. Block copolymers with a low content of β -cyclodextrin still show similar curves to the statistical block copolymer as depicted in

Figure 6. The LCST is slightly lower than the statistical block copolymer owing to the reduced presence of TMSPA, hence, subsequently, yielding a lower β -cyclodextrin content. Block copolymers prepared with a higher TMSPA feed ratio, however, did not possess a visible LCST and the scattering intensity remain unaffected over the range of temperatures measured.

Table 2. Summary of Block Copolymers Obtained Using POEGMEA₄₀-macro-RAFT with Different Ratios of TMSPA and NIPAAM after Polymerizing for 20 h

feed ratio	% convn ^a	calculated composition from conversion	cum F_{TMSPA} (theor cum F_{TMSPA}) ^b	before deprotection		after deprotection and CD modification	
				$M_{n,\text{theo}}/\text{g mol}^{-1}$	$M_{n,\text{GPC}}/\text{g mol}^{-1}$ (PDI) ^c	$M_{n,\text{theo}}/\text{g mol}^{-1}$	$M_{n,\text{GPC}}/\text{g mol}^{-1}$ (PDI) ^c
$f_{\text{TMSPA}} = 0.05$	64	POEGMEA ₄₀ - <i>b</i> -P(NIPAAM ₁₅₀ - <i>s</i> -TMSPA ₁₁)	7% (7.4%)	38 150	35500 (1.65)	50 150	57500 (1.56)
$f_{\text{TMSPA}} = 0.1$	62	POEGMEA ₄₀ - <i>b</i> -P(NIPAAM ₁₃₇ - <i>s</i> -TMSPA ₁₈)	11% (14.2%)	38 000	33000 (1.55)	57 550	65000 (1.51)
$f_{\text{TMSPA}} = 0.2$	56	POEGMEA ₄₀ - <i>b</i> -P(NIPAAM ₁₁₅ - <i>s</i> -TMSPA ₂₄)	17% (29%)	36 570	27000 (1.51)	62 700	54000 (1.59)

^a overall conversion of both monomers. ^b Cumulative composition of the P(TMSPA-*s*-NIPAAM) block at the listed conversion calculated using the reactivity ratios in Table 1 (CONTOUR) for RAFT (Figure S6, Supporting Information, for graph). ^c DMAc, measured against PS standards.

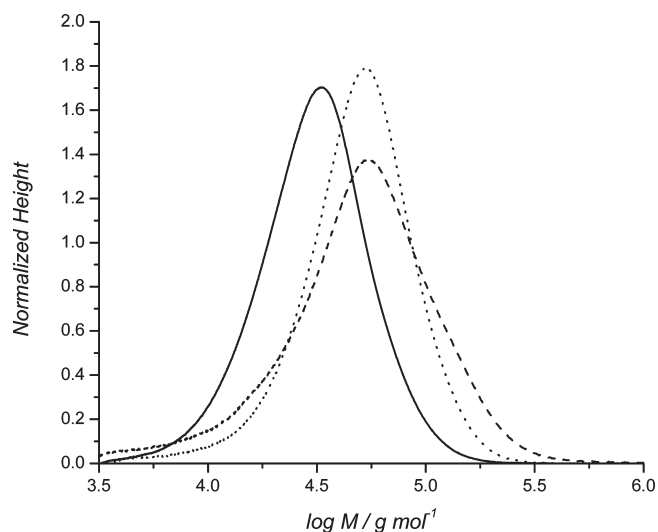


Figure 6. SEC traces of POEGMEA-*b*-P(NIPAAM-*s*-PA) before reaction (—), POEGMEA-*b*-P(NIPAAM-*s*-PA) clicked with 6I-azido-6I-deoxy- β -cyclodextrin using copper catalyst at 140 °C for 30 min (\cdots), and POEGMEA-*b*-P(NIPAAM-*s*-PA) modified with β -cyclodextrin azide at 100 °C for 24 h (----).

This may be explained by the absence of phase separation between both blocks. While it is expected that above the LCST, POEGMA and PNIPAAM form two immiscible blocks, it also needs to be considered that cyclodextrin undergo inclusion complex formation with many polymers including poly(ethylene oxide) (PEO), although α -cyclodextrin is more suitable for the inclusion complex formation with PEO.^{51–54} A range of hydrogels have been generated using this approach,^{54,55} although hydrogels from PEO and cyclodextrin only are not very stable in the presence of high amount of water.⁵⁴ This host–guest formation could force the hydrophilic PEO into the PNIPAAM environment shifting the LCST to values above the measured range. Evidence can be found in the aggregate formation below the LCST. Theoretically, below the LCST, aggregate formation should be absent due to the water-solubility of both blocks. However, all block copolymers listed in Table 3 show small round particles of diameters of 10–15 nm under the TEM accompanied by a large fraction of undefined large particles with 100–500 nm (Figure 8). Above the LCST and the dehydration of PNIPAAM, the formation of micelles with sizes of around 40 nm (TEM) or 50 nm (DLS) takes place. Aggregate formation

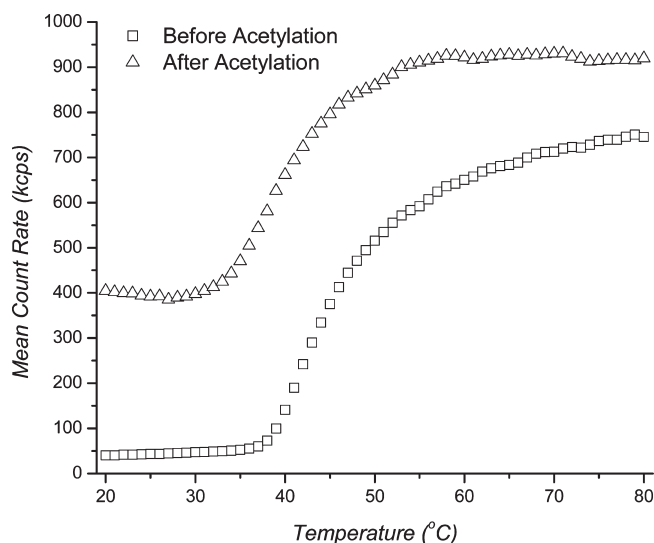


Figure 7. Scattering intensity vs temperature of POEGMEA₄₀-*b*-P(NIPAAM₁₅₀-*s*-PA- β -cyclodextrin₁₁), before and after acetylation, in water.

below the LCST may not only be caused by inclusion complex formation, but also by the formation of strong hydrogen bonding between two cyclodextrin molecules, a process that is especially prevalent with polymers that contain higher concentrations of cyclodextrin moieties.⁵⁰

For further variation of the LCST, the hydroxyl groups of β -cyclodextrin were acetylated using a standard procedure. As a result, the hydrophilicity of the building block was lowered, which is reflected by a LCST of 34 °C but also by a strong tendency to form a high fraction of micelles with a hydrodynamic diameter of 100 nm even at room temperature. At the LCST, the core of the micelles collapses forming particles of 30 nm.

Albendazole Drug Loading and Cell Toxicity Tests. The insolubility of albendazole in water ($2.00 \times 10^{-4} \text{ g L}^{-1}$ or $7.57 \times 10^{-6} \text{ mol L}^{-1}$)⁵⁶ requires the consumption of vast amounts of drug to treat any diseases in a meaningful way. Cyclodextrins have been chosen earlier to address the low water-solubility.^{10,57,58} phase diagrams have been studied in detail confirming the formation of 1:1 complexes between β -cyclodextrin^{10,58} while NMR analysis suggest inclusion via the propyl group as depicted in Figure 1.¹⁰ Although the ABZ-CD complex has been thoroughly studied in literature with a range of techniques, NMR studies are

Table 3. LCST Values Determined Using DLS (Scattering Intensity) before and after ABZ Loading

sample	polymer composition	F/%	LCST/°C	LCST (after ABZ loading)/°C	$K_{1:1}/\text{L mol}^{-1}$
1	β -cyclodextrin	-	-	-	$1600 \pm 5\%$
2	P(NIPAAAM ₁₁₆ - <i>s</i> -PA- β -cyclodextrin ₄₃)	27	42	46	$1600 \pm 5\%$
3	POEGMEA ₄₀ - <i>b</i> -P(NIPAAAM ₁₅₀ - <i>s</i> -PA- β -cyclodextrin ₁₁)	7	38	42	$3950 \pm 5\%$
4	POEGMEA ₄₀ - <i>b</i> -P(NIPAAAM ₁₃₇ - <i>s</i> -PA- β -cyclodextrin ₁₈)	11	-	>55	$3950 \pm 5\%$
5	POEGMEA ₄₀ - <i>b</i> -P(NIPAAAM ₁₁₅ - <i>s</i> -PA- β -cyclodextrin ₂₄)	17	-	>55	$4200 \pm 5\%$
6	POEGMEA ₄₀ - <i>b</i> -P(NIPAAAM ₁₅₀ - <i>s</i> -PA- β -acetyl-cyclodextrin ₁₁)	7	34	48	$37000 \pm 5\%$

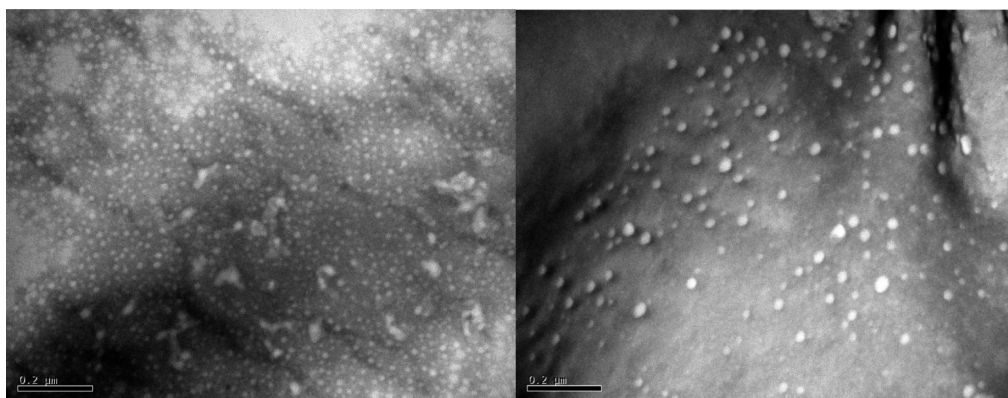


Figure 8. TEM images of block copolymer POEGMEA₄₀-*b*-P(NIPAAAM₁₅₀-*s*-PA- β -cyclodextrin₁₁) particles using phosphotungstic acid negative staining at 25 °C (left) and 55 °C (right).

limited. In most cases, the shift of β -cyclodextrin signals have been monitored, but also the ABZ signals underwent some changes. As seen in Figure S8, Supporting Information, confirming various studies in literature, the ^1H NMR signals corresponding to cyclodextrin is dependent on the amount of albendazole added with the largest changes occurring at a 1:1 molar ratio between β -CD and ABZ (ESI, Figure S8, Supporting Information). The structure of the complex as shown in Figure 1 has been derived from the shift of the propyl signals of ABZ.¹⁰ The aliphatic protons were shielded in the presence of β -CD, but it is not clear to what extent the aromatic group may be involved. However, so far no two-dimensional rotating frame NOE spectroscopy (ROESY)⁵⁹ has been carried out to elucidate the structure of the host–guest complex. However, even after many attempts, we failed to obtain suitable cross peaks and the formation of the complex was only characterized by establishing the phase-solubility diagram. The apparent binding constant between ABZ and β -cyclodextrin was calculated from this diagram using a method developed by Higushi and Connors.¹⁰ The apparent binding constant $K_{1:1} = \text{slope}/S_0(1 - \text{slope})$ was obtained from the slope of the linear relationship between cyclodextrin concentration and the amount of encapsulated ABZ and the initial solubility of ABZ in the absence of cyclodextrin S_0 . Values of $K_{1:1}$ for this inclusion complex formation was reported as 1382 L mol^{-1} ⁵⁸ and 965 L mol^{-1} (3.643 mL mg^{-1}).¹⁰ Loading was usually achieved by mixing an aqueous cyclodextrin solution with ABZ, which is dissolved in an organic solvent such as THF or acetone. After incubation, the organic solvent was removed under vacuum and excess ABZ was filtered off. Using this approach, we obtained a slightly higher value for the inclusion complex formation with $K_{1:1} = 1600 \text{ L mol}^{-1}$ (Table 3). The loading capacity was not affected when the statistical copolymers P(NIPAAAM-*s*-PA- β -cyclodextrin) were

tested. The apparent binding constant of 1600 L mol^{-1} was obtained with the polymer listed in Table 3, but also with other copolymers prepared with different feed ratios (Figure 3), therefore loading was not affected by the cyclodextrin content in the polymer, in contrast to other work where the interaction was reduced when CD was conjugated to a polymer.⁶⁰ On the contrary, the block copolymers with POEGMA lead to double the ABZ loading. This can be understood by the role of PEG chains to contribute to the overall enhancement of the solubility of ABZ delaying precipitation of ABZ when the organic solvent is removed from aqueous system. A significant jump in the complex formation can be observed after acetylation (Table 3). The effect of the modification of hydroxyl groups on the complex formation has been discussed earlier.^{61,62} Acetylation will affect the size of the cavity and also the type of forces between CD and drug.⁶³

The drug is encapsulated via the hydrophobic tail while the more hydrophilic part is exposed to the outside. This exposed part of the drug molecule can now manipulate the overall hydrophilicity of the PNIPAAAM copolymer influencing the LCST.^{24,35} The measured LCST values were observed to be slightly increased owing to the presence of the hydrophilic carbamate part of the drug ABZ (Table 3). The drug molecule also imparts now stimuli-responsive properties to the block copolymers with higher β -cyclodextrin content while a visible LCST was absent in the absence of ABZ. Drug loading obviously facilitates phase separation between PNIPAAAM and the POEGMA block. The changes in the LCST in the acetylated polymer were much more pronounced due to the much higher loading of ABZ.

The ABZ loaded polymers were tested as drug delivery carriers. The statistical copolymer and the block copolymer are tested against β -cyclodextrin in their performance. The aim is to have a nontoxic carrier while the drug-carrier system should show

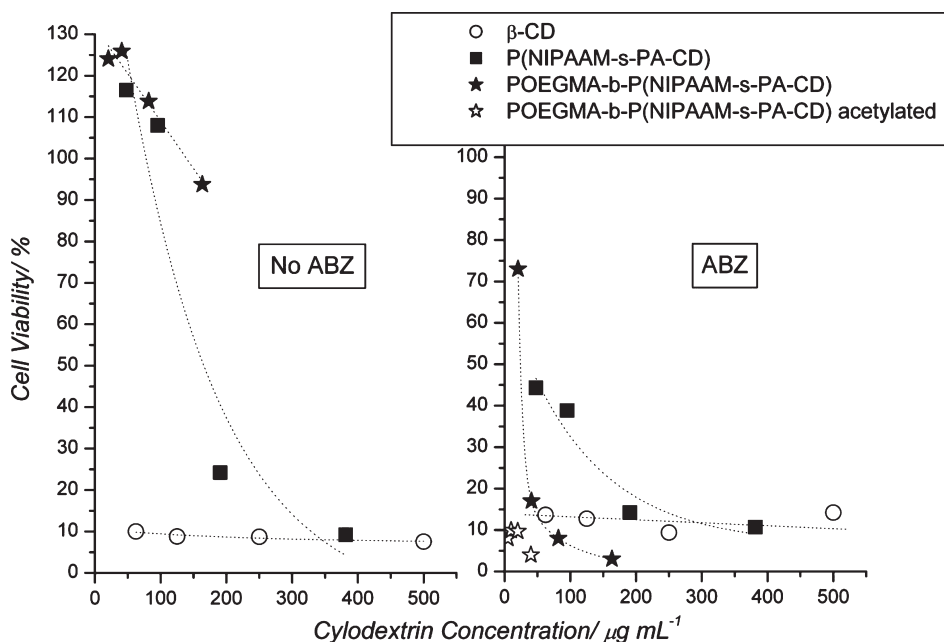


Figure 9. Cell viability test using OVCAR-3 ovarian cancer cell lines with β -cyclodextrin, statistical copolymer P(NIPAAM₁₁₆-s-PA- β -cyclodextrin₄₃), and the block copolymer POEGMA₄₀-b-P(NIPAAM₁₅₀-s-PA- β -cyclodextrin₁₁) and the acetylated block copolymer before ABZ loading (left) and after ABZ loading (right).

high cytotoxicity. It should be noted here that the block copolymer is not expected to form micelles under these conditions. LCST values seem to suggest that the polymers are water-soluble at the cell test temperature of 37 °C. In addition, the stability of block copolymer micelles is highly challenged in cell growth media resulting often in disaggregation.³⁴ However, the presence of PEG can increase biocompatibility and possibly enhance cellular uptake of the drug carrier. Results from preliminary studies have suggested that ABZ is an efficient anticancer drug against ovarian cancer.⁸ OVCAR-3 cell lines were chosen to test the activity of the ABZ loaded systems. Parent (unmodified) β -cyclodextrin, statistical copolymer, and block copolymer were tested for toxicity against cell lines before and after ABZ loading. Initially, the biocompatibility of β -cyclodextrin and its polymers were tested on viable OVCAR-3 cells. Figure 9 shows the percentage viability of OVCAR-3 cell relative to the control sample after 72 h incubation at 37 °C with four different vectors concentration of 62.5, 125, 250, and 500 $\mu\text{g mL}^{-1}$, which is equivalent to different amounts of cyclodextrin. Therefore, the cell viability was recorded against the concentration of cyclodextrin (Figure 9). β -cyclodextrin alone was found to be toxic to cells, even when unloaded with drug. This has been observed earlier^{64–67} and the toxicity of β -cyclodextrin may be attributed to its uptake by cells, leading to the disruption of intracellular function or the extraction of lipid membrane components such as cholesterol and phospholipids.⁶⁵ The statistical copolymer also showed its toxicity as the concentration increased while the block copolymer, with its PEG chains counterbalanced the toxicity of β -cyclodextrin.

The polymers were subsequently loaded with ABZ. Vectors concentration, incubation time, and temperature were the same as before. Even after ABZ loading, the statistical copolymer was more toxic than the block copolymer. ABZ loaded β -cyclodextrin is as cytotoxic as β -cyclodextrin alone resulting in more than 90%

cell death. An interesting result was obtained when comparing two polymers. Although the complex formation constant between ABZ and β -cyclodextrin in the block copolymer is slightly higher, the overall amount of cyclodextrin is lower in this system. As a consequence, the amount of ABZ encapsulated by the same vector concentration is lower in POEGMA₄₀-b-P(NIPAAM₁₅₀-s-PA- β -cyclodextrin₁₁). However, the cytotoxicity of the block copolymer is significantly higher leading to more than 90% cell death even at low concentration.

A remarkable effect is observed using the acetylated polymer. Even very small concentrations lead to more than 90% of cell death. This drug carrier is therefore highly effective owing to the higher ABZ loading, but could also have other origins.

To understand these effects further studies are warranted. The increased toxicity may be the preferred cellular uptake of carriers carrying PEG moieties by the cell, but further studies, including drug-release rates, are needed to understand this effect.

CONCLUSION

A biocompatible drug delivery system has been created which combines the host–guest complexation of β -cyclodextrin with the possibility of targeting a tumor passively by employing polymers. The host–guest complexation between the drug albendazole and the cyclodextrin carrying polymer was highly dependent on the fine-structure of the polymer. Loading efficiencies affected the performance of the drug carrier but also the LCST of the PNIPAAm block. Higher loading led to increased cytotoxicity but also to increased LCST values since the host–guest complex mainly buries the hydrophobic part of the drug while the hydrophilic part is exposed. The cytotoxicity results can potentially be correlated to the loading capacity but more studies are needed to fully understand how the structure of the polymer affects drug release and cellular uptake.

■ ASSOCIATED CONTENT

S Supporting Information. Evolution of M_n vs the conversion, pseudo-first order kinetic plots, characteristics of homopolymers and random copolymers ^1H NMR and FTIR spectra, calculation of polymer composition FNIPAAm and FTMSPA from NMR, molecular weight distribution obtained from SEC, and calculated cumulative polymer composition. This material is available free of charge via the Internet at <http://pubs.acs.org>.

■ AUTHOR INFORMATION

Corresponding Author

*Corresponding author. E-mail: m.stenzel@unsw.edu.au.

■ ACKNOWLEDGMENT

M.H.S. thanks the ARC (Australian Research Council) for a Future Fellowship (FT0991273) and funding for this project (DP110102409). The authors also thank the staff from the NMR facility (Jim Hook, Dr Donald Thomas) at UNSW for their help and support. F.Y. also acknowledges Ministry of Higher Education Malaysia for sponsoring his doctorate studies.

■ REFERENCES

- (1) Pourgholami, M. H.; Akhter, J.; Wang, L.; Lu, Y.; Morris, D. L. *Cancer Chemother. Pharmacol.* **2005**, *55* (5), 425–432.
- (2) Pourgholami, M. H.; Woon, L.; Almajd, R.; Akhter, J.; Bowery, P.; Morris, D. L. *Cancer Lett. (Shannon, Ireland)* **2001**, *165* (1), 43–49.
- (3) Morris, D. L.; Jourdan, J.-L.; Pourgholami, M. H. *Oncology* **2001**, *61* (1), 42–46.
- (4) Hossein Pourgholami, M.; Cai, Z. Y.; Lu, Y.; Wang, L.; Lawson Morris, D. *Clin. Cancer Res.* **2006**, *12* (6), 1928–1935.
- (5) Khalilzadeh, A.; Wangoo, K. T.; Morris, D. L.; Pourgholami, M. H. *Biochem. Pharmacol.* **2007**, *74* (3), 407–414.
- (6) Jung, H.; Medina, L.; Garcia, L.; Fuentes, I.; Moreno-Esparza, R. *J. Pharm. Pharmacol.* **1998**, *50* (1), 43–48.
- (7) Pourgholami, M. H.; Wangoo, K. T.; Morris, D. L. *Anticancer Res.* **2008**, *28* (5A), 2775–2779.
- (8) Kim, Y.; Pourgholami, M. H.; Morris, D. L.; Stenzel, M. H. *Macromol. Bioscience* **2011**, *11* (2), 219–233.
- (9) Szejtli, J. *Pure Appl. Chem.* **2004**, *76* (10), 1825–1845.
- (10) Joudieh, S.; Bon, P.; Martel, B.; Skiba, M.; Lahiani-Skiba, M. *J. Nanosci. Nanotech.* **2009**, *9* (1), 132–140.
- (11) Uekama, K.; Hirayama, F.; Irie, T. *Chem. Rev.* **1998**, *98* (5), 2045–2076.
- (12) Evrard, B.; Chiap, P.; DeTullio, P.; Ghalmi, F.; Piel, G.; Van Hees, T.; Crommen, J.; Losson, B.; Delattre, L. *J. Controlled Release* **2002**, *85* (1–3), 45–50.
- (13) Cheng, J.; Khin, K. T.; Davis, M. E. *Mol. Pharmaceutics* **2004**, *1* (3), 183–193.
- (14) Ramirez, H. L.; Valdivia, A.; Cao, R.; Torres-Labandeira, J. J.; Fragoso, A.; Villalonga, R. *Bioorg. Med. Chem. Lett.* **2006**, *16* (6), 1499–1501.
- (15) Skiba, M.; Bounoure, F.; Barbot, C.; Arnaud, P.; Skiba, M. *J. Pharm. Pharmacol. Sci.* **2005**, *8* (3), 409–418.
- (16) Pun, S. H.; Bellocq, N. C.; Liu, A.; Jensen, G.; Machemer, T.; Quijano, E.; Schlupe, T.; Wen, S.; Engler, H.; Heidel, J.; Davis, M. E. *Bioconjugate Chem.* **2004**, *15* (4), 831–840.
- (17) Zhang, J.-T.; Huang, S.-W.; Zhuo, R.-X. *Macromol. Chem. Phys.* **2004**, *205* (1), 107–113.
- (18) Yhaya, F.; Gregory, A. M.; Stenzel, M. H. *Aust. J. Chem.* **2010**, *63* (2), 195–210.
- (19) Furue, M.; Harada, A.; Nozakura, S. *J. Polym. Sci., Polym. Lett. Ed.* **1975**, *13* (6), 357–60.
- (20) Liu, Y.-y.; Fan, X.-d.; Gao, L. *Macromol. Biosci.* **2003**, *3* (12), 715–719.
- (21) Carbonnier, B.; Janus, L.; Deratani, A.; Morcellet, M. *J. Appl. Polym. Sci.* **2005**, *97* (6), 2364–2374.
- (22) Gonzalez, H.; Hwang, S. J.; Davis, M. E. *Bioconjugate Chem.* **1999**, *10* (6), 1068–1074.
- (23) Cheng, J.; Khin, K. T.; Jensen, G. S.; Liu, A.; Davis, M. E. *Bioconjugate Chem.* **2003**, *14* (5), 1007–1017.
- (24) Amajjahe, S.; Choi, S.; Munteanu, M.; Ritter, H. *Angew. Chem., Int. Ed.* **2008**, *47* (18), 3435–3437.
- (25) Amajjahe, S.; Munteanu, M.; Ritter, H. *Macromol. Rapid Commun.* **2009**, *30* (11), 904–908.
- (26) Seo, T.; Kajihara, T.; Iijima, T. *Makromol. Chem.* **1987**, *188* (9), 2071–82.
- (27) Perrier, S.; Takolpuckdee, P. *J. Polym. Sci., Part A: Polym. Chem.* **2005**, *43* (22), 5347–5393.
- (28) Favier, A.; Charreyre, M. T. *Macromol. Rapid Commun.* **2006**, *27* (9), 653–692.
- (29) Moad, G.; Rizzardo, E.; Thang, S. H. *Aust. J. Chem.* **2009**, *62* (11), 1402–1472.
- (30) Moad, G.; Thang, S. H. *Aust. J. Chem.* **2009**, *62* (11), 1379–1381.
- (31) Stenzel, M. H. *Chem. Commun.* **2008**, *30*, 3486–3503.
- (32) Stenzel, M. H. *Macromol. Rapid Commun.* **2009**, *30* (19), 1603–1624.
- (33) Gregory, A.; Stenzel, M. H. *Expert Opin. Drug Delivery* **2011**, *8* (2), 237–269.
- (34) Kim, S.; Shi, Y. Z.; Kim, J. Y.; Park, K.; Cheng, J. X. *Expert Opin. Drug Delivery* **2010**, *7* (1), 49–62.
- (35) Maciollak, A.; Munteanu, M.; Ritter, H. *Macromol. Chem. Phys.* **2010**, *211* (2), 245–249.
- (36) Stenzel, M. H.; Davis, T. P. *J. Polym. Sci., Part A: Polym. Chem.* **2002**, *40* (24), 4498–4512.
- (37) Stenzel, M. H.; Cummins, L.; Roberts, G. E.; Davis, T. P.; Vana, P.; Barner-Kowollik, C. *Macromol. Chem. Phys.* **2003**, *204* (9), 1160–1168.
- (38) Harvey, D. F.; Lund, K. P.; Neil, D. A. *J. Am. Chem. Soc.* **1992**, *114* (22), 8424–34.
- (39) Malkoch, M.; Thibault, R. J.; Drockenmuller, E.; Messerschmidt, M.; Voit, B.; Russell, T. P.; Hawker, C. J. *J. Am. Chem. Soc.* **2005**, *127* (42), 14942–14949.
- (40) Ladmiral, V.; Mantovani, G.; Clarkson, G. J.; Cauet, S.; Irwin, J. L.; Haddleton, D. M. *J. Am. Chem. Soc.* **2006**, *128* (14), 4823–4830.
- (41) Khan, A. R.; Forgo, P.; Stine, K. J.; D'Souza, V. T. *Chem. Rev.* **1998**, *98* (5), 1977–1996.
- (42) Munteanu, M.; Choi, S.; Ritter, H. *Macromolecules* **2008**, *41* (24), 9619–9623.
- (43) Zhang, L.; Bernard, J.; Davis, T. P.; Barner-Kowollik, C.; Stenzel, M. H. *Macromol. Rapid Commun.* **2008**, *29* (2), 123–129.
- (44) vanHerk, A. M. *CONTOUR (v1.8)*.
- (45) vanHerk, A. M.; Droge, T. *Macromol. Theory Simul.* **1997**, *6* (6), 1263–1276.
- (46) Feldermann, A.; Toy, A. A.; Phan, H.; Stenzel, M. H.; Davis, T. P.; Barner-Kowollik, C. *Polymer* **2004**, *45* (12), 3997–4007.
- (47) Pai, T. S. C.; Barner-Kowollik, C.; Davis, T. P.; Stenzel, M. H. *Polymer* **2004**, *45* (13), 4383–4389.
- (48) Quemener, D.; Le Hellaye, M.; Bissett, C.; Davis, T. P.; Barner-Kowollik, C.; Stenzel, M. H. *J. Polym. Sci. Part A: Polym. Chem.* **2008**, *46* (1), 155–173.
- (49) Schild, H. G. *Prog. Polym. Sci.* **1992**, *17* (2), 163–249.
- (50) Choi, S.; Munteanu, M.; Ritter, H. *J. Polym. Res.* **2009**, *16* (4), 389–394.
- (51) Tonelli, A. E. *Macromolecules* **2008**, *41* (11), 4058–4060.
- (52) Tonelli, A. E. *Polymer* **2008**, *49* (7), 1725–1736.
- (53) Harada, A.; Kamachi, M. *Macromolecules* **1990**, *23* (10), 2821–2823.
- (54) van de Manakker, F.; Vermonden, T.; van Nostrum, C. F.; Hennink, W. E. *Biomacromolecules* **2009**, *10* (12), 3157–3175.
- (55) Zhu, W.; Li, Y.; Liu, L.; Chen, Y.; Wang, C.; Xi, F. *Biomacromolecules* **2010**, *11* (11), 3086–3092.

(56) Evrard, B.; Chiap, P.; DeTullio, P.; Ghalmi, F.; Piel, G.; Van Hees, T.; Crommen, J.; Losson, B.; Delattre, L. *J. Controlled Release* **2002**, *85* (1–3), 45–50.

(57) Kata, M.; Shauer, M. *Acta Pharm Hung* **1991**, *61*, 23.

(58) Moriwaki, C.; Costa, G. L.; Ferracini, C. N.; de Moraes, F. F.; Zanin, G. M.; Pineda, E. A. G.; Matioli, G. *Braz. J. Chem. Eng.* **2008**, *25* (2), 255–267.

(59) Rojas-Aguirre, Y.; Yépez-Mulia, L.; Castillo, I.; López-Vallejo, F.; Soria-Arteche, O.; Hernández-Campos, A.; Castillo, R.; Hernández-Luis, F. *Bioorg. Med. Chem.* **2011**, *19* (2), 789–797.

(60) Weickenmeier, M.; Wenz, G. *Macromol. Rapid Commun.* **1996**, *17* (10), 731–736.

(61) Gelb, R. L.; Schwartz, L. M. *J. Inclusion Phen.* **1989**, *7* (5), 537–543.

(62) Zhang, B. L.; Breslow, R. *J. Am. Chem. Soc.* **1993**, *115* (20), 9353–9354.

(63) Rekharsky, M. V.; Inoue, Y. *Chem. Rev.* **1998**, *98* (5), 1875–1917.

(64) Irie, T.; Uekama, K. *J. Pharm. Sci.* **1997**, *86* (2), 147–162.

(65) Stella, V. J.; Rajewski, R. A. *Pharm. Res.* **1997**, *14* (5), 556–567.

(66) Brewster, M. E.; Loftsson, T. *Adv. Drug Delivery Rev.* **2007**, *59* (7), 645–666.

(67) Loftsson, T.; Brewster, M. E. *J. Pharm. Pharmacol.* **2010**, *62* (11), 1607–1621.